Supporting Information

Akashi et al. 10.1073/pnas.1003878107

SI Materials and Methods

Collection of Hair Follicle Cells. Healthy volunteers were asked to follow a set schedule for at least 1 wk. Wake-up time and meal times were set based on the lifestyle habits of each subject. The subjects were asked to have breakfast, lunch, and dinner about 1, 6, and 13 h after waking up in the morning, respectively. They were also asked to refrain from consuming excess alcohol, eating excessive snacks, and taking long naps. Each subject wore an Actiwatch on their nondominant wrist to objectively ascertain behavioral rhythms. Hair follicle cells were collected by firmly holding and pulling the root of scalp hair, and hair follicle cells (the cells attached to the hair roots) were quickly soaked in dissolution buffer (RNeasy Micro Kit; QIAGEN). Hair follicle cells were stored at −70 °C until RNA purification. At each sampling point, about 10 male hair follicle cells (scalp hair) and about 20 female hair follicle cells (scalp hair) were required. Sufficient amounts of RNA can also be obtained using five facial hair follicle cells. When collecting scalp hairs, samples were obtained from different regions of the scalp. Although there may be individual and racial differences in yield, hairs from the tip of the chin tend to yield a greater amount of RNA. The RNeasy Micro Kit (QIAGEN) was used with frozen cytolysis solution to purify total RNA. After checking the quality and concentration of total RNA using a Bioanalyzer (Agilent) or NanoDrop (LMS), samples were used to determine clock gene mRNA. The present study was approved by the Ethical Review Board of Saga University, and informed consent was obtained from each subject.

Animals. Mice were housed using a strict 12 h/12 h light/dark regimen. Tissues were immediately frozen in liquid nitrogen and stored at −80 °C until processed for RNA. All protocols for experiments using animals in this study were approved by the Saga University Animal Research Committee. Quantification of relative RNA levels was performed with SYBER Green real-time PCR technology as described previously (1). Briefly, DNase-treated total RNA (2.5 μg) was reverse-transcribed using an oligo(dT) primer and SuperScript reverse transcriptase (Invitrogen). The cDNA equivalent of 20 ng of total RNA was PCR-amplified in a PRISM 7300 detection system (Applied Biosystems).

mRNA Determination. Total RNA was reverse-transcribed using ReverTra Ace (Toyobo), and real-time PCR was performed using a TaqMan MGB probe (Applied Biosystems) and 1/20 volume of the reverse-transcription product. Data were obtained using a PRISM 7300 (Applied Biosystems) and corrected by 18S rRNA. Primers were selected when there was no unspecific amplification in dissociation curves and when amplification efficiency was relatively favorable. FAM-MGB (a 6-carboxyfluorescein fluorescent dye and a minor groove binding) labeling was carried out on designed matching probes. The sequences of the primers and probe for each human gene are shown in Dataset S1. In addition, as a technique for determination differing from real-time PCR, RNA determination was performed using branched-DNA probes (QuantiGene; Panomics). With this method, total RNA purification, reverse transcription, and PCR amplification are not required, and target mRNA is thus directly detected in cytolysis solutions. This RNA determination technique differs markedly from real-time PCR. Data were corrected by *Pp1a* levels.

Microarray Experiments. At each sampling point, about 20 scalp hairs were collected. Total RNA was prepared using the RNeasy Micro Kit (QIAGEN). After checking the quality and concentration of total RNA using a Bioanalyzer (Agilent) and NanoDrop (LMS), samples were used for microarray experiments. One hundred and fifty nanograms of total RNA was amplified and labeled using the Affymetrix Whole-Transcript (WT) Sense Target Labeling Protocol without rRNA reduction. Affymetrix GeneChip Human Gene 1.0 ST arrays were hybridized with 11 μg of labeled sense DNA, washed, stained, and scanned according to the protocol described in the WT Sense Target Labeling Assay Manual. Affymetrix GeneChip software was used to determine the average difference between perfectly matched oligonucleotide probes and single-base-pair mismatches for each probe set. Data were then scaled globally to make the total intensity of each microarray equal. The resulting hybridization intensity values reflect the abundance of a given mRNA relative to the total RNA population and were used in all subsequent analyses.

Genes with significant changes were screened by one-way ANOVA of 2 d of microarray expression profiles with a P value threshold of 0.1, counting 2-d data as duplicate data of a day, followed by a permutation test to evaluate significance in circadian rhythmicity of each gene expression. These time-course gene expression data are normalized by their root-mean-squares and randomly permuted 10,000 times to calculate P values of fast Fourier transform (FFT) and cosine fitting correlation (CF) analysis of the data. Correlation P value of CF analysis was calculated as the ratio of the number of permutation correlations, calculated from nonlinear least-squares fitting of a 24-h-period cosine curve to the data, that had higher correlation value than the nonpermuted data to the number of tested permutation data. P value of FFT analysis was calculated as the ratio of the number of permutation data that had higher 24-h-period power of FFT analysis than nonpermuted data to the number of tested permutation data. Obtained P values were used to filter genes by false discovery rate (FDR) of $\alpha = 0.05$.

Cosine Curve Fitting of Experimental Data. A 24-h-period cosine curve (Eq. **S1**) was fitted by the nonlinear least-squares method to the time-course gene expression data we obtained, with $E(t)$ indicating gene expression level at time t, A indicating the amplitude of the cosine curve, ω indicating the phase, and C indicating the offset value. Fitted curves were used for mathematical representation of rhythms of gene expression for comparison with predicted rhythm curves.

Prediction of Rhythm of Expression from Three-Point Experimental Data. Gene expression rhythm curves for *Per3* and *Nr1d2* were predicted as follows: First, the levels of gene expression of *Per3* and *Nr1d2* at time t, $E(t)per3$ and $E(t)nr1d2$, were modeled as in Eq. **S2**, where A indicates amplitude, ω indicates the *Per3* phase, C indicates the offset value, and θ indicates the phase difference, and subscripts are gene names. Phase difference between *Per3* and *Nr1d2* was set to an experimental value, the mean of *Per3* and *Nr1d2* phase differences of 17 healthy volunteers. Each phase difference was calculated from fitted cosine curves of *Per3* and *Nr1d2*. Next, the model equations (Eq. **S2**) were fitted to the target three-point experimental data using the conjugate gradient minimization method. Model parameters were determined by minimizing the sum of squares of differences between experimental data and equation values at the same time points. Initial values of A and C for the method were set to the amplitudes of standard curves described later and the mean of the

target three-point data, respectively. The initial value of the *Per3* phase parameter ω was set to each hour of the day, and the resulting curves yielding the minimum sum of squares of differences were chosen as those for predicted rhythm of expression for target three-point data.

Determination of Optimal Sampling Interval. To ascertain optimal sampling time intervals for stable and accurate prediction, we examined our method of prediction using various sampling intervals and start times. First, a cosine curve was fitted to actual measurements obtained from each of 13 healthy volunteers, and 24 combinations of hypothetical sampling times were set for each hour of the day. Three sampling time points were selected based on target time intervals, and the above three-point prediction was applied. Means and SEs of the phase time differences between the predicted curves and the cosine fitted curves were calculated for each of the 24 combinations of sampling starting time. Results showed that the optimal sampling interval for our 3-h-interval experimental data was a 6 h-6 h interval.

Prediction of Rhythm of Expression from Three-Point Experimental Data by Standard Curve Fitting. Improvement of the accuracy of prediction was performed using fixed amplitudes and offsets in a fitting model for three-point prediction (Eq. **S2**). First, a cosine curve was fitted to actual measurements obtained from each of the six healthy volunteers. Mean amplitude and offset of the fitted curves for each gene were set to fitting model parameters (Eq. **S2**) and used as "standard curves." Next, the standard curves were fitted to three-point measured data by the nonlinear least-squares method to determine *Per3* phase ω, with the initial value set to each hour of the day. The resulting curves with the lowest SEs were selected as those for prediction of rhythm of gene expression for three-point data.

Cross-Validation. To evaluate the validity of the standard-curve method, 6-fold cross-validation was performed. Among sampling data of six normal individuals which were used to define parameters of the standard curve, five were used as a training dataset to define the standard curve and the remaining one was used as test data to estimate the phase by the standard curve. This was performed for all possible combinations of the six individuals and phase estimation errors were calculated from them.

Simulation. To examine the limit of three-point phase prediction for rhythms that vary from the standard curve, phase prediction errors for randomly generated rhythm data were examined. Generally, circadian rhythm is approximated by a 24-h-period cosine curve, and therefore Per3 and Nr1d2 rhythm data are generated based on cosine curves. Parameters of the cosine curve, amplitude, phase, and oscillation offset are randomly set, centered to those of the standard curve. Ten thousand cosine curves with different sets of parameters are generated, and these curves are then used to generate 12 three-point sampling data of different sampling start times with 6 h-6 h sampling intervals. The phase of Per3 was fixed to 6 h and the phase of Nr1d2 was randomly set to have a phase difference around that of the standard curve, 2.1 h. Randomly generated datasets are then performed phase prediction by fitting standard curves, and phase prediction errors are calculated (see "Prediction of Rhythm of Expression from Three-Point Experimental Data by Standard Curve Fitting" in *SI Materials and Methods*).

Prediction of Rhythm of Expression from Single-Point Experimental Data by Standard Curve Fitting. Phase predictions of single-point data were achieved by an extension of the three-point data prediction method using nine gene standard curves (*Bmal1*, *Rev-erbα*, *Rev-erbβ*, *Per1*, *Per2*, *Per3*, *Cry1*, *Npas2*, and *DBP*) for prediction. A cosine curve was fitted to the time course of gene expression in each tissue obtained from three mice, and its amplitude and offset were used for the gene expression standard curve. We assumed a fixed phase difference among the selected genes in each tissue, and the phase differences of standard curves were obtained from the fitted cosine curves. As in the case of phase prediction of three-point data by standard curve fitting, those nine standard curves were fitted to single-time-point data for expression of nine genes by the nonlinear least-squares method. To avoid biasing of results due to exponential differences between expression values, each measured datum and standard curve were weighted by the inverse of the amplitude of the corresponding standard curve. The resulting curves with the lowest SEs were selected as those for the prediction of rhythm of gene expression for single-point data.

$$E(t) = A\cos\left\{\frac{2\pi(t+\varpi)}{24}\right\} + C \qquad \textbf{[S1]}$$

$$\begin{aligned}\text{Per3}: E_{per3}(t) &= A_{per3}\cos\left\{\frac{2\pi(t+\varpi)}{24}\right\} + C_{per3}\\ \text{Nr1D2}: E_{nr1d2}(t) &= A_{nr1d2}\cos\left\{\frac{2\pi(t+\varpi+\theta)}{24}\right\} + C_{nr1d2}\end{aligned} \qquad \textbf{[S2]}$$

SI Result 1

Phase differences exist in rhythms of expression among clock genes, and such phase intervals were stable. Using the phase interval for phase prediction, we focused on *Per3* and *Nr1d2*, whose expression rhythm data could consistently be obtained from human hair follicle cells and exhibited small individual differences in phase interval (Fig. 2*B*). To accurately calculate the phase interval, rhythms of expression of *Per3* and *Nr1d2* were investigated in 17 healthy subjects (Fig. S7*A*). The peak times for *Per3* and *Nr1d2* were determined by fitting a cosine curve using the nonlinear least-squares method. Results showed that the average phase difference for *Per3* and *Nr1d2* was 2.2 ± 0.097 h. Although marked individual differences were observed in the phases of rhythm of expression, the phase interval appeared stable for *Per3* and *Nr1d2*. This was also the case for shift workers (white circles) and a subject who habitually exercised vigorously at night (gray circles). Using phase differences, the rhythm of expression of *Per3* and *Nr1d2* was fitted to a 24-h cosine curve (*SI Materials and Methods*; Eq. **S2**). A indicates amplitude, ω indicates *Per3* phase, C indicates offset value, and θ indicates phase difference, and subscripts are gene names. Because *Per3* phases were used to indicate *Nr1d2* phases, the two model formulae included five unknown constants. To mathematically deduce these unknown constants, five independent equations are needed. Because a single two-gene assay could yield two equations using the model formulae, at least three samplings were required with the present model. We therefore attempted to predict the phases of rhythm of expression by collecting samples at three different time points.

SI Result 2

When predicting rhythmic variations of gene expressions using three-point data, accuracy of prediction is dependent on sampling interval. Because marked individual differences exist in phases of rhythm of expression (Fig. S7*A*), all possible sampling start times around the clock need to be considered. We thus performed three-point phase prediction with various sampling intervals and start times to ascertain the optimal sampling time interval (Fig. S7*B*). A cosine curve was fitted to actual measurements obtained for each of 13 healthy volunteers, and 24 hypothetical sampling times were set for each hour of the day. Based on the resulting model data, three sampling time points were selected based on target time intervals, and unknown constants that best fit model Eq. **S2** (*SI Materials and Methods*) were determined using the

conjugate gradient method. This was performed for all 24 sampling starting times to assess accuracy of prediction. In this fashion, means and SEs of the time difference between predicted and model phases were calculated for each sampling time interval. Although the results indicated high accuracy of prediction for many sampling time intervals (e.g., 6 h-6 h and 3 h-3 h intervals), three-point prediction was not successful with some sampling time intervals (e.g., 9 h-15 h interval). Accuracy of prediction was highest with the sampling time interval of 8 h-8 h.

SI Result 3

Fig. S9*A* shows the results for 3 h-3 h intervals (seven three-point combinations). As with subject C, when all data were close to the cosine curve, accuracy of prediction was sufficiently high with a 3 h-3 h interval, whereas with subject D, when a deviating value was observed, accuracy of prediction was lower than with a 6 h-6 h interval. With this standard-curve method, the degree of tolerance for data fluctuations and errors is high, and highly accurate yet flexible prediction is possible. Because errors and fluctuations are unavoidable in actual gene expression measurements in clinical settings, the technique using the standard curve is superior to the above-noted conjugate gradient method. However, because gene expression is assumed to follow the standard curve, the standard-curve method cannot be applied to data quantified with PCR calibration curves deduced by a dilution series of different calibration samples. Constant calibration samples for real-time PCR must always be used when measuring gene expression. When analyzing data indicating markedly low expression (almost always due to insufficient RNA extraction), the correlation of three measurements to the standard curve will be low (see the value next to the phase time in Fig. 4 and Fig. S9*A*). These cases can be excluded or distinguishable as "unmeasurable" or "unhealthy." In the future, the accuracy of phase prediction can be further improved by identifying available genes other than *Per3* and *Nr1d2*, and prediction may be possible using only two time points.

We explored the possibility of single-point phase prediction using expression data for nine clock genes obtained from mouse peripheral tissues (Fig. S9*B*). Five peripheral tissues were collected from three mice every 4 h around the clock (six time points), and nine clock gene expressions were examined. The average cosine curve prepared using these data were defined as the standard curve. Thirty combinations of single-point prediction (five tissues and six time points) were performed based on expression data for the nine clock genes, and phase prediction was successful in most cases tested. The maximum error in relation to the six-point calculated curve was about 2.6 h, although errors were within 1.5 h in most cases. These findings indicate that one- or two-point phase prediction is possible for human data with our standard-curve method using more genes whose rhythms of expression are consistently detectable in hair follicle cells.

SI Discussion. Although the methodology presented here could be useful for studying the human circadian clock, there is room for further improvements. First, the number of hairs required for measurement could be reduced. In men, it can be reduced to fewer than five hairs if beard hair is substituted for head hair, although other improvements will be needed to characterize the circadian clock in women with a smaller number of hairs. Additionally, although we used a general real-time PCR or bDNA-based assay for mRNA quantification in this study, more sensitive methods of RNA detection should be considered to reduce the number of hairs required. In our experience, the number of cells attached to a plucked hair root appears to be dependent to some extent on the method used to pluck hair, and further optimization of this method will be required. Related to this, we found that there is a positive correlation between the force used to pluck hairs and the amount of total RNA extracted from hairs (Fig. S2 *A* and *B*). This correlation may allow efficient collection of hairs and lead to a reduction in the number of hairs required. To achieve this, we have manufactured trial pen-shaped hair tweezers which allow us to select hairs that are firmly rooted (Fig. S2*C*). Although our model is based only on two or three clock genes that were rhythmically expressed with a clear circadian pattern, the accuracy of prediction of circadian phase by three-point sampling could be improved if other clock genes are used. We recently adopted a strategy allowing us to perform multigene expression profiling with simple experimental processes, because the procedures used for detection in this study are technically difficult for high-throughput analysis of a large number of samples. Specifically, rapid multigene expression profiling from many specimens can be performed with the combination of the Luminex instrument system (Hitachi) and bDNA-based mRNA quantification (Fig. S3). If these improvements could be achieved, our hair-based detection method will markedly contribute not only to basic research on the human circadian clock but also to the clinical diagnosis of circadian rhythm disorders.

1. Akashi M, Takumi T (2005) The orphan nuclear receptor RORα regulates circadian transcription of the mammalian core-clock Bmal1. *Nat Struct Mol Biol* 12:441–448.

A

	CF	FFT
Total Selected	220	251

B

	CF	FFT
Per3	1	1
Nr1d1	4	12
Nr1d2	6	16
Per1	27	27

Fig. S1. Genes with significant circadian rhythms were selected from microarray gene expression data. Fast Fourier transform (FFT) and cosine fitting correlation (CF) followed by a permutation-derived *P* value assessment were performed for 10,000 permuted datasets generated from time-course gene expression data of 2,823 genes that were prescreened by ANOVA of the microarray gene expression data. The *P* values were then used to screen genes with significant circadian rhythms by the FDR of $\alpha = 0.05$. (*A*) The number of genes selected by CF and FFT. (*B*) Ranks of clock genes in the selected gene list.

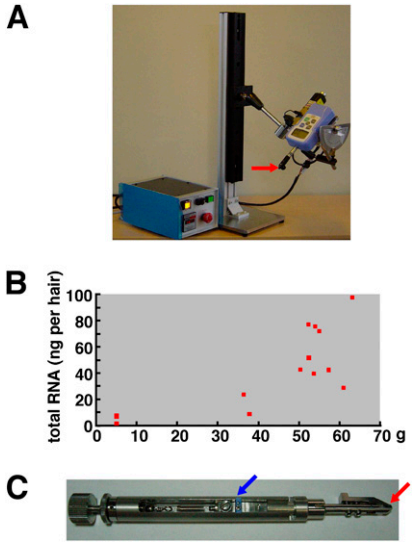

Fig. S2. Efficient methods for hair sample selection. (*A*) A device that measures the force necessary to pluck head hair samples was developed. Holding a hair with the tip of the device (red arrow), the force can be measured by pulling it by electric motor. (*B*) Using the device shown in *A*, the correlation between total RNA extraction and hair removal force was investigated. In the subject shown, head hair samples could be collected efficiently by selecting hairs that required at least 50 g of force to pluck. (*C*) A pen-type device that can easily measure the force to pluck a head hair was developed. Holding a hair with the tip (red arrow), the blue bar (blue arrow) slides depending on tensile force and stops when the hair is removed. The force required to pluck can be ascertained based on the location of the blue bar, and the device can be used for efficient hair sample selection.

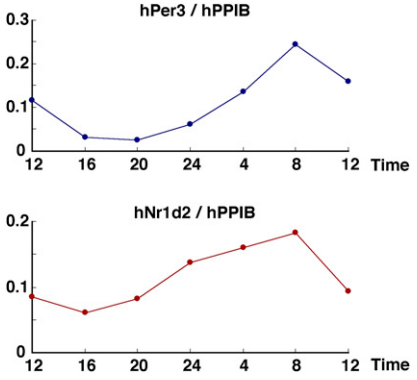

Fig. S3. A high-throughput method of detection of rhythms of clock gene expression. Five facial hairs were collected every 4 h, and the expression of clock (*Per3* and *Nr1d2*) and correction (*PPIB*) genes was measured by quantitative RNA analysis using QuantiGene Plex (Panomics). With this system, each well contains three beads to which branched DNA to detect *Per3*, *Nr1d2*, or *PPIB* mRNA is fixed. A single test can thus simultaneously measure three gene expressions. After allowing each sample to react, the solution is removed from each well, and the Luminex system (Hitachi) is used to measure signals. The figures show expression of the clock genes (*Per3* and *Nr1d2*) corrected by *PPIB*. Application of this technique can increase measurement throughput for determination of rhythms of clock gene expression.

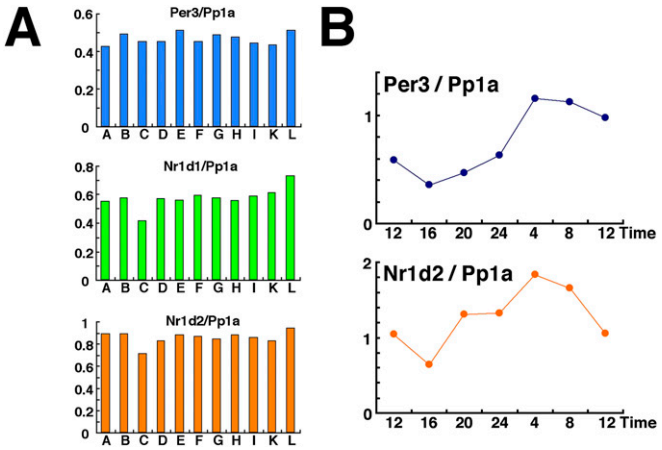

Fig. S4. Expression of clock genes in facial hair follicle cells. (*A*) Expression of clock genes in facial hair follicle cells was measured by RNA determination using branched DNA. This method differs markedly from real-time PCR, because RNA purification, reverse transcription, and PCR amplification are not required. Eleven samples of three facial hairs were collected to assess fluctuations in measurement. Clock gene levels were normalized to *Protein Phosphatase 1 A* (*Pp1a*). (*B*) Time-course sampling of facial hairs was carried out, and rhythms of clock gene expression were measured using the branched-DNA method.

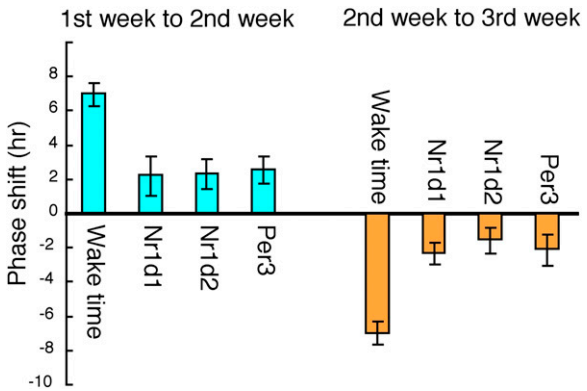

Fig. S5. The average phase shift of wake time and circadian gene expression was calculated among the six subjects in Fig. 3. The phase delay from the first to the second week and the phase advance from the second to the third week are shown.

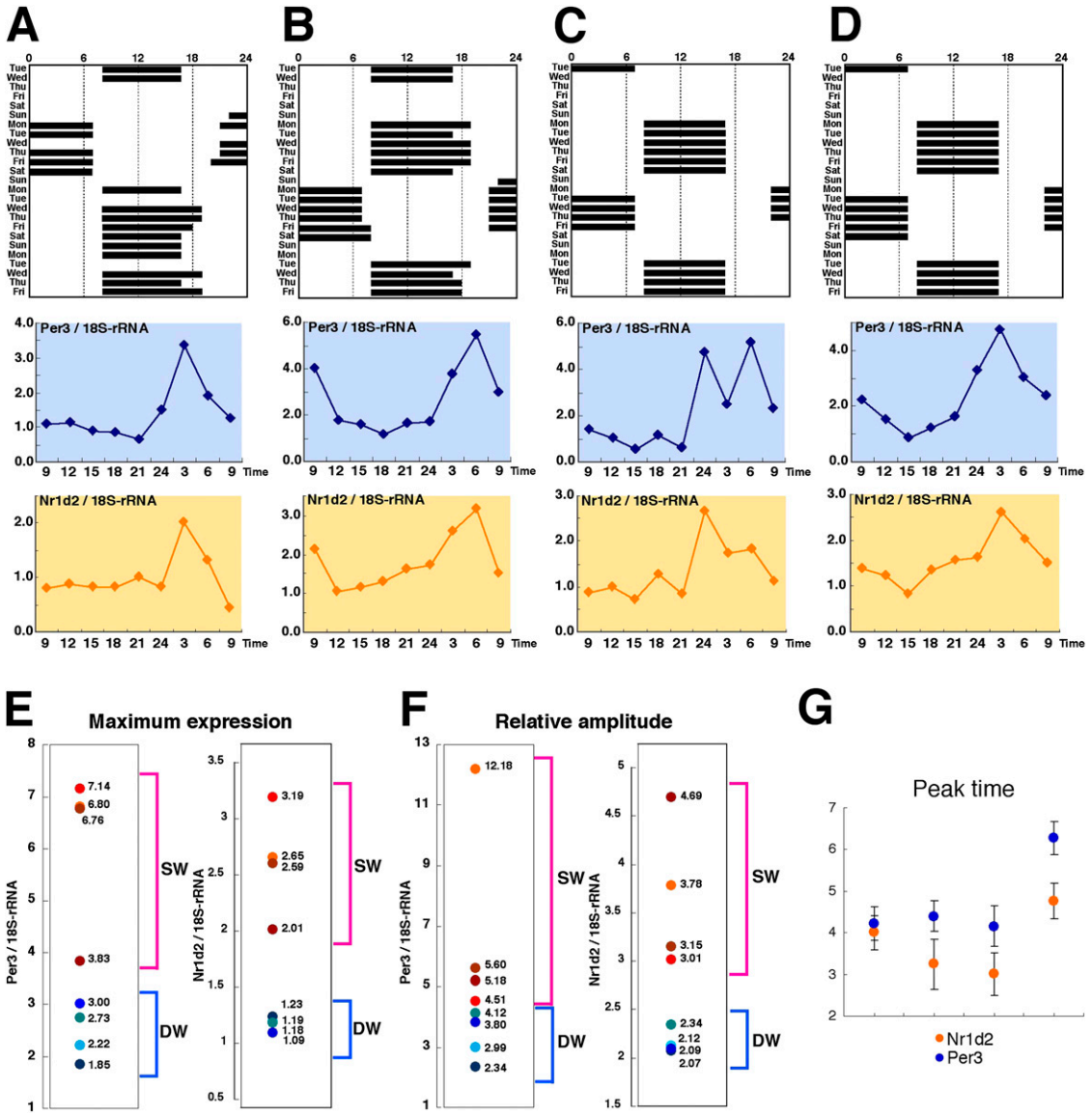

Fig. S6. Rhythms of clock gene expression in rotating shift workers. We observed a higher oscillation amplitude and maximum expression of circadian clock gene expression compared with daytime workers when experiments were performed with another set of subjects with a different work schedule. (*A*–*D*) For four rotating shift workers, a work shift table (upper figure) and clock gene expression (lower figures) are shown. The final day in the schedule is the sampling day. Scalp hair samples were collected every 3 h to ascertain rhythms of clock gene expression by real-time PCR. Expressions relative to 18S rRNA are shown. (*E* and *F*) Peak values (*E*) and relative amplitudes (*F*) of clock gene expression rhythms were calculated, and the results were compared among four rotating shift workers and four healthy individuals. For precise comparison between normal subjects and rotating shift workers, clock gene expression in all eight subjects was measured under the same experimental conditions and with the same types of handling. SW and DW indicate shift workers and daytime workers, respectively. (*G*) Cosine curve fitting was applied to clock gene expression rhythm data for each subject, and peak times were calculated.

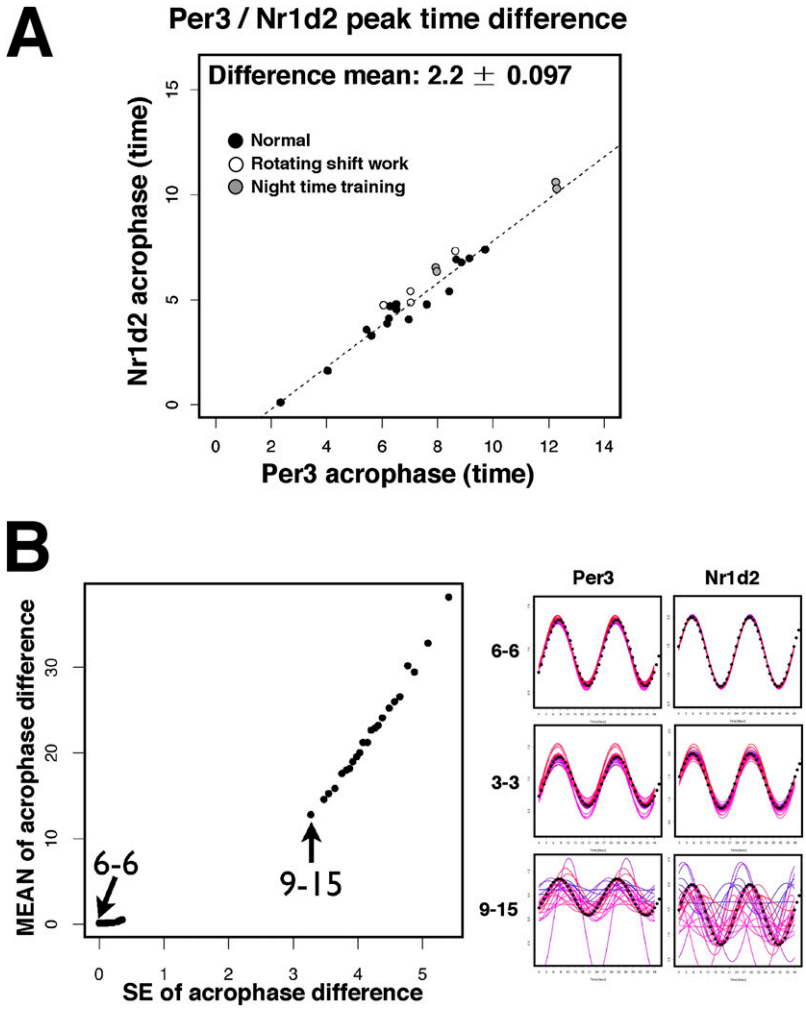

Fig. S7. (*A*) To ascertain the peak time difference between *Per3* and *Nr1d2*, the peak time of each gene was plotted for 17 healthy volunteers (black dots). Cosine fitting was undertaken for time-series expression data for *Per3* and *Nr1d2* obtained using scalp or facial hair samples, and time of maximum expression for *Per3* was plotted on the *x* axis and *Nr1d2* on the *y* axis. The broken line shows the average for peak time difference (2.2 h). White circles indicate the four shift workers, and gray circles indicate the subject who habitually exercised vigorously at night (the two delayed phases are with exercise). (*B*) (*Left*) Determination of the ideal three-point sampling time interval for optimal phase prediction. Cosine fitting was performed for rhythms of *Per3* and *Nr1d2* expression measured using scalp or facial hair samples, and hypothetical sampling times were set for each hour of the day. For each sampling time interval combination (for example, 6-6 indicates three samplings with sequential 6-h intervals), the phase time difference between the model and three-point prediction curve (24 combinations) was calculated. Average phase difference was plotted on the *y* axis, while average SE was plotted on the *x* axis. The same analysis was performed for 13 healthy volunteers, and the average was calculated. (*Right*) Waves predicted based on three-point assays. The results of prediction for 24 combinations of sampling starting times are shown for the 6 h-6 h interval (upper), 3 h-3 h interval (middle), and 9 h-15 h interval (lower). The broken black line indicates the model curve, black dots indicate hypothetical sample collection times established along the model curve, and color lines indicate three-point prediction curves for the 24 combinations.

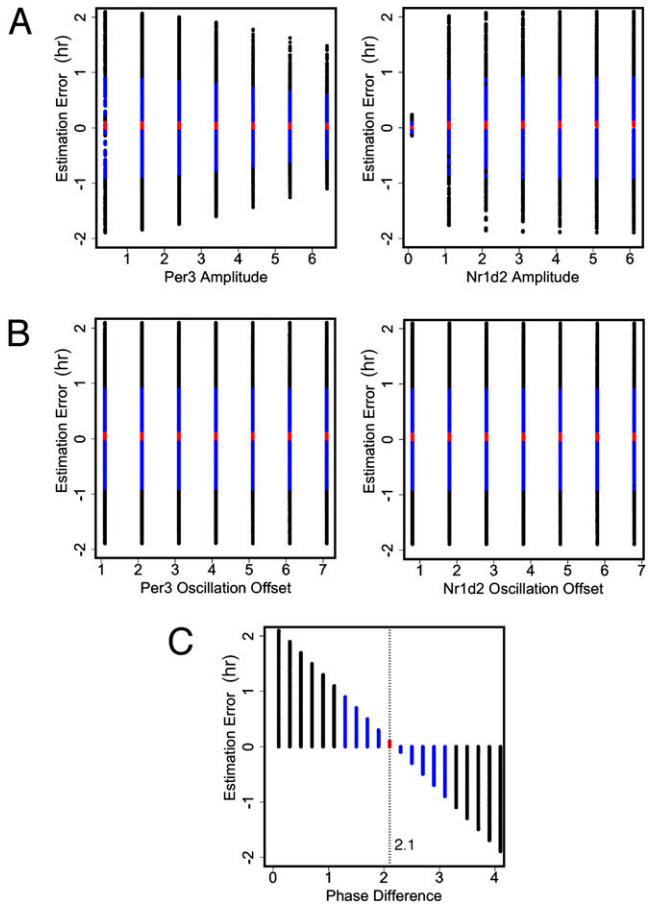

Fig. S8. One hundred and twenty thousand combinations of three-point sampling data, based on cosine curves with randomized set amplitude, phase, and oscillation offset, were generated and three-point phase predictions were performed. (*A*) The phase prediction results in terms of amplitude of *Per3* and *Nr1d2* expression rhythms. The *x* and *y* axes are the relative amplitude and prediction error in hours, respectively. (*B*) The phase prediction results in terms of oscillation offset values of *Per3* and *Nr1d2* expression rhythms. The *x* and *y* axes are the relative oscillation offset value and prediction error in hours, respectively. (*C*) The phase prediction results in terms of the phase difference between *Per3* and *Nr1d2*. The *x* and *y* axes are the phase difference and prediction error in hours, respectively. The red dots are the results of expression rhythms with the fixed *Per3-Nr1d2* phase difference of 2.1 h, whereas the blue ones are those with phase differences between 1.1 and 3.1 h.

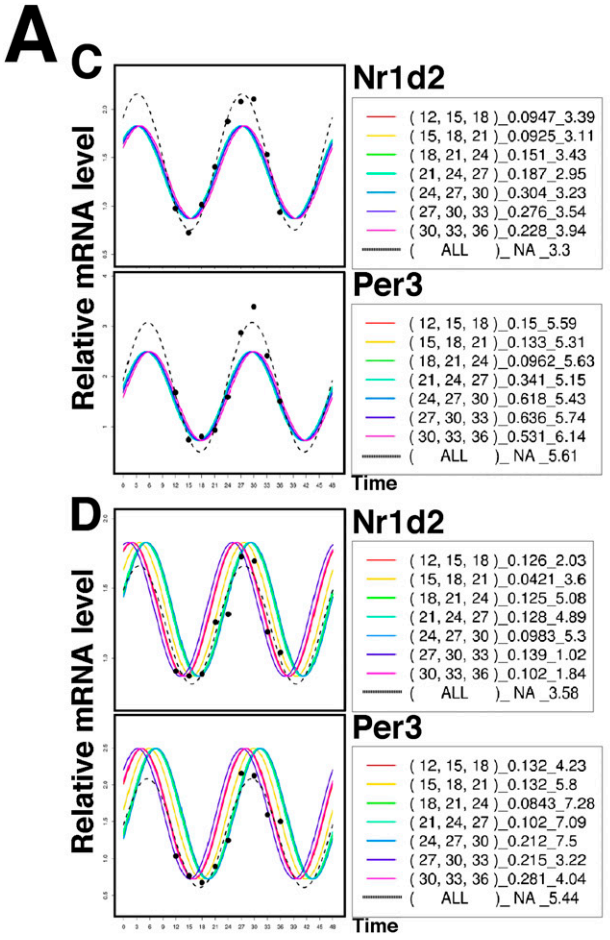

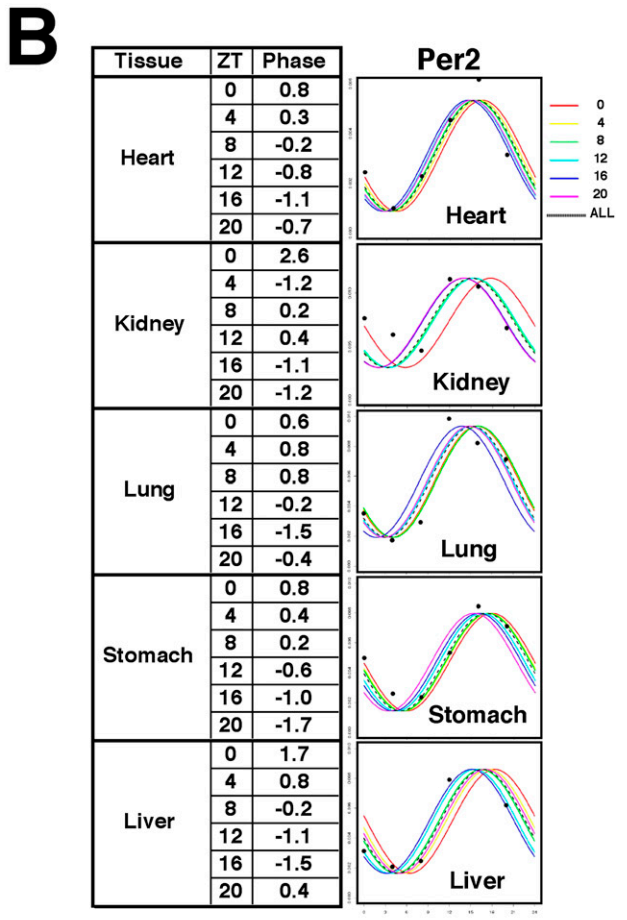

Tissue	ZT	Phase
Heart	0	0.8
	4	0.3
	8	-0.2
	12	-0.8
	16	-1.1
	20	-0.7
Kidney	0	2.6
	4	-1.2
	8	0.2
	12	0.4
	16	-1.1
	20	-1.2
Lung	0	0.6
	4	0.8
	8	0.8
	12	-0.2
	16	-1.5
	20	-0.4
Stomach	0	0.8
	4	0.4
	8	0.2
	12	-0.6
	16	-1.0
	20	-1.7
Liver	0	1.7
	4	0.8
	8	-0.2
	12	-1.1
	16	-1.5
	20	0.4

Fig. S9. (*A*) Three-point phase prediction using actual data. Phase prediction was performed using the standard curve for the three-point assay with sampling time intervals of 3 h-3 h. The standard curve refers to the average cosine curve prepared using actual data. Factors other than phase time, such as period, amplitude, levels of expression, and the phase interval between *Per3* and *Nr1d2*, were fixed. Black dots indicate actual measurements, the broken black line indicates a curve calculated based on all nine-point data (ALL), and colored lines indicate three-point predicted curves. Subjects C and D in Fig. 4 and Fig. S9*A* are the same individuals. Numbers in parentheses beside figures indicate the time points of the three samplings used for prediction (actual data were obtained at nine points every 3 h, and three of the nine points were selected), and numbers at the right indicate root-mean-square errors of three-point prediction curves and three measurements (the smaller the value, the more accurate the prediction). Additionally, numbers on the right show predicted peak times. The closer the nine-point calculated phase to the three-point predicted phase, the more accurate the prediction. (*B*) Single-point phase prediction using expression data obtained from mouse peripheral tissues. Five peripheral tissues were collected from three mice every 4 h, and average levels of expression were calculated at every time point for nine clock genes. A cosine curve was fitted to time-series average data and defined as the standard curve, whose wave elements other than phases were fixed when performing prediction (the phase interval among the nine clock genes was also fixed). The standard curve varies in peripheral tissues. Thirty combinations of single-point prediction (five tissues and six time points) were performed based on expression data for nine clock genes. "Phase" represents the phase time difference between the six-point calculated and single-point predicted curve; the smaller the absolute value (h), the more accurate the prediction. The right figure shows the predicted curves for *Per2* expression as examples. ZT represents Zeitgeber time.

Other Supporting Information Files

Dataset S1. A list of circadian rhythm genes isolated by comprehensive gene expression analysis (FFT) of hair follicle cells. The table presents the names of the rhythm gene clusters shown in Fig. 1*B*. They are ranked in order of FDR values. The Probe ID column shows the GeneChip probe ID number (Affymetrix).

Dataset S1